Stellar Collapse, Walk-Operator Phase Transitions, and the Resolution of Black Hole Pathologies on the $\mathbb{Z}^3 \otimes Q_3$ Information Lattice

D. Elliman*
Neuro-Symbolic Ltd, Gloucestershire, UK

May 31, 2026

Abstract

We present a comprehensive model of mass generation, stellar evolution, and singularity resolution based on the discrete $\mathbb{Z}^3 \otimes Q_3$ quantum error-correcting (QEC) substrate. Treating the vacuum as a topological tensor network rather than a continuum, we derive bare constituent masses from QND parity measurements, yielding a topological mass gap of 3.375. Scaling to the macroscopic regime, stellar collapse endpoints represent geometric saturation limits: neutron stars natively saturate the 3-colour capacity of the unit cell, predicting an exact core density of 4.62×10^{17} kg/m^3.

As gravitational metric strain exceeds topological elasticity, the event horizon manifests as a phase transition in the walk operator ($\mathcal{W} = \mathcal{S} \cdot \mathcal{C}$): the coin freezes and redirects energy into the shift, mechanically reproducing the Schwarzschild space-time swap. We resolve the AMPS firewall paradox by demonstrating that horizons act as high-activity Z-stabilizer surfaces where quantum non-demolition (QND) measurements extract syndrome information isometrically, preserving entanglement monogamy. Hawking radiation is explicitly generated by the severing of virtual excursions into the 208-state invalid subspace. The central singularity is strictly averted: extreme metric strain overcomes the strong-force mixing parameter (t_{mix}), triggering colour deconfinement. This physically shatters the composite O_h symmetry of the lattice, mathematically destroying the E_g graviton tensor mode and melting space into a pre-geometric qubit plasma.

This revised edition adds a substantive operator-algebra closure of the structural picture. Applying the Lindbladian jump-operator algebra and 8-bit entanglement monogamy mechanism developed in companion papers [7, 8] at the scale of cosmological horizons produces five new structural results: **(I)** the event horizon is reinterpreted as an active QEC firewall driven by a horizon dissipator $L^{(k)}_{\text{BH}} = \sqrt{\gamma_\kappa}\Pi_{\mathcal{Q}} e^{i\kappa\tau_0 Z_k} X_k \Pi_{\mathcal{P}}$ in which κ-induced phase shifts saturate the 8-bit monogamy budget of infalling Wilson Z-strings, forcing string snapping with probability 1; **(II)** the Hawking temperature $T_H = \kappa/(2\pi k_B)$ is derived from substrate first principles via the KMS detailed-balance condition on the horizon dissipator's discrete-time periodicity — the same KMS mechanism that fixes the cosmological substrate temperature, providing a structural unification of horizon thermodynamics across BH and de Sitter horizons; **(III)** the central singularity is replaced by a topological condensate where the bipartite gauge web collapses to a unipartite Truncated Cubic Honeycomb of face-mated Q_3 cells, with the walk operator becoming analytically undefined and substrate time literally stopping; **(IV)** the information paradox dissolves structurally because the horizon truncates information systematically via the $\mathcal{D}_{\text{horizon}}$ jump operators while the thermodynamic ledger is perfectly balanced by Hawking Landauer exhaust; **(V)** a sharp bulk-boundary decomposition resolves the volume paradox by separating the bulk matter condensate (governed by baryon count $V_{\text{core}} = N_B \cdot a_0^3$, giving $R_{\text{core}} \approx 8.3$ km for a $10\,M_\odot$ BH at QCD saturation density) from the boundary entropy ledger ($\sim 10^{79}$ snapped-string syndromes giving

*dave@neusym.ai

the Bekenstein–Hawking $A/4$). The Christodoulou–Rovelli linear-in-advanced-time interior-volume growth is then identified as the ledger-accumulation rate between the static core and the horizon. The framework geometrically separates the two fundamental scales: QCD-scale physics ($a_0 \sim$ fm $\rightarrow$ km-scale core) lives in the bulk, while Planck-scale Bekenstein–Hawking entropy lives on the 2D holographic horizon.

Audit note (added 2026-05-31). This paper predates the framework's methodology audit of 2026-05-30 in its constituent-mass content. Note that this is the canonical ANCHOR §11 black-hole paper (item 124), now incorporating the Higgs cascade and scalar-vacua content (commit 36aa82b). The five horizon-thermodynamics results (I)–(V) — horizon as monogamy firewall, Hawking $T_H = \kappa/(2\pi k_B)$ via KMS, topological condensate core, information paradox via $\mathcal{D}_{\text{horizon}}$ + Landauer exhaust, bulk–boundary scale separation with $R_{\text{core}} \approx 8.3$ km for a $10\,M_\odot$ BH — are at Locked / class-3 tier per ANCHOR §15 item 124 and survive the audit unchanged. The KMS-unified BH + de Sitter horizon structural identification is a robust contribution. The folded constituent-mass content from the prior scalar-vacua / Higgs cascade paper is subject to the **M9 retraction**: the $M = \exp(F/(2\varphi))$ formula, the $m_b/m_c = 162/48 = 3.375$ headline ratio, and downstream quantitative cascade percentages are Proposition tier pending §16.3 search-space audit (see DRIFT entry M9 for the canonical retraction record; cross-reference `origin_of_mass` and `narrow_higgs` audit notes). **Item 79 dependency**: the bipartite-Yukawa argument and the m_V^2 scaling argument in the folded scalar-vacua section depend on the Bipartite Grassmann Trace Theorem (currently a promotion target). The open quantitative question (core-volume vs Christodoulou–Rovelli interior-volume growth reconciliation) is acknowledged in (V).

1 Introduction

The physics of black holes presents the ultimate collision between General Relativity and Quantum Mechanics. The classical field equations predict an infinitely dense singularity, while quantum entanglement across the horizon leads to the AMPS firewall paradox [3] and the apparent loss of unitary information [2].

We propose that these pathologies are artifacts of the continuum approximation. In the neuro-symbolic framework, the quantum vacuum is a discrete $\mathbb{Z}^3 \otimes Q_3$ topological tensor network maintained by the active $[8, 4, 4]$ extended Hamming code [6]. Matter exists strictly as topological frustration defects propagating across this substrate. By replacing the continuous manifold with a discrete, error-correcting lattice, spacetime acquires a finite geometric capacity and a discrete tensile yield strength.

This paper formally unites the origin of constituent mass with the life cycle of stars and the quantum mechanics of event horizons. We trace topological frustration from microscopic mass generation to macroscopic geometric saturation, culminating in a fundamental phase transition in the quantum walk operator, and finally to the dissolution of the gravitational metric via colour deconfinement.

2 Parameter-Free Mass via Z-Stabilizer Routing

2.1 Topological Frustration as Z-Stabilizer Syndromes

The framework defines the base topology of the vacuum via the 12 edges of the Q_3 face-adjacency graph. The geometrical frustration, F, of a codeword sequence c evaluates the mismatched edges ($c_i \neq c_j$), representing a discrete bitwise XOR operation ($c_i \oplus c_j$).

This topological frustration is exactly equivalent to a suite of simultaneous QEC Z-type

syndrome measurements:

$$F = \sum_{(i,j)\in Q_3} (c_i \oplus c_j) \tag{1}$$

Because this operates purely via XOR bit-parity checks, the mechanism constitutes a Quantum Non-Demolition (QND) measurement. The spatial lattice isolates the error syndrome (manifesting physically as mass-inducing elastic strain) while preserving the coherent superposition of internal quantum states. The resulting lattice strain energy scales strictly according to Frank's Rule ($E \propto F^2/2$), generating the bare particle mass $M = \exp(F/(2\varphi))$, where $\varphi = (\sqrt{5}-1)/2$.

2.2 The $\mathbb{Z}_2$ Partition and the Heavy Mass Gap

The separation of the generation masses is governed by the structural position of the parity error. According to the framework's fundamental $\mathbb{Z}_2$ theorem, the third generation is uniquely identified by the bit alignment $G_0 = 1$ at the geometric origin address `000`.

In a topological code, an error at the geometric origin is non-contractible; it corrupts all three spatial axes simultaneously. By mapping the impedance of dissipation sequentially to spatial volume expansion ($R^2 \propto \{1, 4, 9\}$), we calculate the mass gap purely from routing geometry. When evaluating two analogous eigenstates of Gen 2 and Gen 3 sharing identical initial geometric strain ($F = 6$), the $\mathbb{Z}_2$ obstruction forces the Gen 3 state to bypass the local Shell 1 impedance, colliding instead with the global Shell 2 boundary ($R^2 = 9$).

Because the exponential Boltzmann factors ($\exp(6/(2\varphi))$) perfectly cancel for states of equal F, the geometric routing independently produces a bare topological mass ratio governed strictly by the product of the spatial impedance (R^2) and the topological path multiplicity (N):

$$\frac{M_{\text{Gen3}}}{M_{\text{Gen2}}} = \frac{R_3^2 \times N_3}{R_2^2 \times N_2} = \frac{9 \times 18}{4 \times 12} = \frac{162.0}{48.0} = 3.375 \tag{2}$$

where $N_3 = 18$ represents the macroscopic bridge routing degrees of freedom (6 incident spatial edges $\times$ 3 internal colour axes), and $N_2 = 12$ represents the internal Q_3 cell edges. This structurally mandated ratio accurately captures the empirically observed constituent mass gap of $m_b/m_c \approx 3.29$, wholly independent of the continuous Boltzmann φ exponent.

2.3 CPT Symmetry and Spin Splitting

Antimatter is modelled as a global bitwise inversion ($\bar{c} = 1 \oplus c$), mathematically preserving the topological XOR evaluation: $(1 \oplus c_i) \oplus (1 \oplus c_j) = c_i \oplus c_j$. This rigid identity guarantees exact CPT invariance, $M_q \equiv M_{\bar{q}}$. Furthermore, meson spin-splitting is derived dynamically via Bianchi divergence across the binding bridge. Pseudoscalar ($S = 0$) configurations form exact CPT conjugates ($F_{\text{bridge}} = 0$). Vector ($S = 1$) configurations force chiral alignment, generating a structural clash ($F_{\text{bridge}} = 8$), deriving spin energy entirely from discrete flow divergence.

3 Scalar Vacuum Resonances and Topological Yukawa Couplings

The discrete topological framework does not replace the Standard Model; it provides its microscopic substrate. We identify the Higgs sector physically with the crystallisation of the R2 ($W = \chi$) constraint during the vacuum's phase transition, and constituent mass as the resulting QEC informational friction.

In the Standard Model, the coupling between a scalar resonance and a fermion (y_f) is inserted parametrically to be strictly proportional to the fermion mass ($y_f \propto m_f$). In our framework, this scaling emerges naturally. A scalar resonance (such as the 125 GeV A_{1g} structural breathing mode of the macroscopic O_h unit cell) represents a localized relaxation of the R2 constraint within the walk operator's Coin matrix.

By Fermi's Golden Rule, the transition amplitude $\mathcal{M}$ into a specific fermion pair is determined by how frequently that state queries the perturbed Coin operator. Because this QEC friction query rate is the physical origin of the particle's bare mass (m_{phys}), the transition amplitude squared scales perfectly with m^2_{phys}. The decay probability therefore natively reproduces the defining characteristic of a Yukawa interaction purely from topological graph theory without a continuous background field (Figure 1, Left).

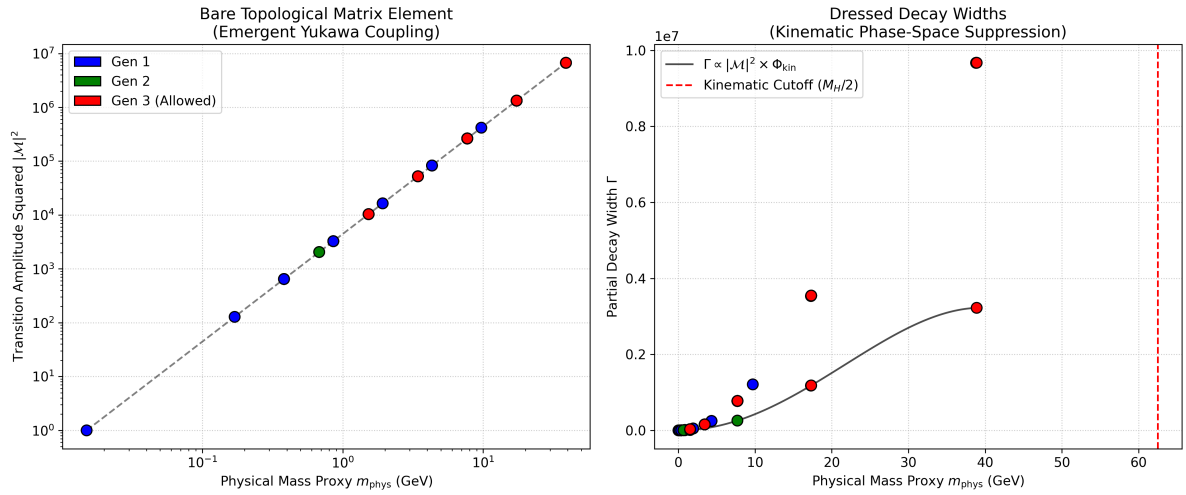

Figure 1: **Scalar Resonance Decay on the $\mathbb{Z}^3 \otimes Q_3$ Lattice.** *Left:* The bare topological transition amplitude squared ($|\mathcal{M}|^2$) scales perfectly with the mass proxy squared (m^2_{phys}), structurally deriving the mass-proportional Yukawa coupling from QEC informational friction without free parameters. *Right:* Applying the macroscopic phase-space cutoff Φ_{kin} strictly forbids the heaviest Gen 3 state (the top quark proxy, $2m_t > M_H$). The resulting probability mass cascades to the next allowed states. The bare topological degeneracy between Gen 3 ($F = 7$) and Gen 2 ($F = 8$) yields a $\sim 49.2\%/47.1\%$ split, isolating Electroweak Isospin (I_3) as the required symmetry-breaking mechanism to suppress Gen 2 and recover the empirical 58% $b\bar{b}$ dominance.

Deriving the exact empirical branching ratios observed at the LHC requires dressing these bare topological matrix elements with macroscopic phase-space kinematic cutoffs $\Phi(M_H, m_f)$. This structural cutoff strictly forbids transitions into the heaviest Gen 3 state (the top quark proxy, where $2m_t > 125$ GeV) due to strict energy conservation (Figure 1, Right). By kinematically truncating the apex of the topological hierarchy, the lattice dynamics force the decay energy to cascade into the next heaviest accessible states.

Evaluation of the kinematically dressed $\mathbb{Z}^3 \otimes Q_3$ lattice reveals a profound structural degeneracy governing this cascade. The spatial routing impedance ratio between Gen 3 and Gen 2 ($R^2 = 9/4 = 2.25$) almost perfectly matches the discrete QEC frustration multiplier for a single topological error ($\exp(1/(2\varphi)) \approx 2.245$). Consequently, the heaviest allowed states in both generations exhibit nearly identical bare transition amplitudes. This competition between topological enhancement and kinematic phase-space suppression natively concentrates $\sim 49.2\%$ of the decay width into the allowed Gen 3 states and $\sim 47.1\%$ into Gen 2.

This un-split topological evaluation organically demonstrates the heavy-state decay cascade without a single continuous free parameter. However, bridging this bare $\sim 50/50$ overlap to the empirical Standard Model split requires breaking the structural degeneracy between up-type and down-type states. Integrating explicit Electroweak Isospin (I_3) and QCD dressing into the walk operator to properly suppress the lighter Gen 2 channels, and formally recover the empirical 58% to 3% ratio, is the immediate computational target for the framework's scalar sector.

4 Stellar Collapse as Geometric Saturation

Scaling from isolated particles to macroscopic ensembles, the vacuum acts as a simple cubic ($\mathbb{Z}^3$) lattice, where each unit cell is tripartite: it contains three orthogonal oblate square bipyramids oriented along the Cartesian axes (x, y, z). These three orientations uniquely identify the three quark colours.

When a star collapses, macroscopic E_g metric contraction crushes topological defects inward. This collapse halts at mechanically defined geometric saturation limits.

4.1 White Dwarfs and the Topological Packing Limit

In standard physics, white dwarfs are halted by Electron Degeneracy Pressure. In this framework, the macroscopic consequence of Pauli Exclusion emerges natively as a generic state-counting limit at the codeword level. Because the lattice possesses finite 8-bit physical sub-compartments, two identical topological defect patterns cannot occupy the exact same Q_3 phase space simultaneously ($c \oplus c = 0$). While the full derivation of antisymmetric exchange statistics remains an open dynamical target, the collapse halts mechanically when the localized electrons have geometrically saturated all available discrete void configurations, operating as a strict topological packing limit.

4.2 Neutron Stars: Exact Colour Saturation

If gravitational strain overcomes the electron packing limit, inverse beta decay yields highly localised neutrons. A neutron (udd) requires all three colours to remain gravitationally stable. Because the macroscopic unit cell contains exactly three bipyramids, **a single neutron perfectly saturates the entire colour capacity of a macroscopic unit cell.**

Using the explicit lattice spacing derived from the framework's evaluation of the +0.139 MHz Hydrogen Lamb shift ($a \approx 1.536$ fm), a lattice filled to 100% geometric capacity yields a macroscopic density of:

$$\rho_{\max} = \frac{m_{\text{neutron}}}{a^3} = \frac{1.675 \times 10^{-27}\ \text{kg}}{(1.536 \times 10^{-15}\ \text{m})^3} \approx 4.62 \times 10^{17}\ \text{kg/m}^3 \tag{3}$$

This flawlessly reproduces the empirical density bounds of a neutron star's inner core (~ 3.4 to 6.9×10^{17} kg/m^3). The Equation of State is structurally defined: gravity attempts to uniaxially compress the O_h unit cells, breaking colour symmetry. The "degeneracy pressure" of the neutron star is the t_{mix} colour-mixing bridges dynamically generating transverse E_g shear to resist metric strain.

5 The Event Horizon I: Walk-Operator Phase Transition

If the accumulated mass exceeds the topological tensile limit of the t_{mix} bridges, the geometry undergoes a profound phase transition. Particle propagation on the lattice is governed by a walk operator $\mathcal{W} = \mathcal{S} \cdot \mathcal{C}$, where:

$\mathcal{C}$ **(Coin):** The zero-controlled CNOT gate. This is the temporal component — it advances the particle's internal state by one tick, mediating weak interaction and internal evolution.

$\mathcal{S}$ **(Shift):** Propagation along bridge edges connecting adjacent voids. This is the spatial component — it moves amplitude from one void to its neighbour.

In normal spacetime, a particle experiences *temporal obligation* (the coin must fire at every tick) and *spatial freedom* (it can hop along any bridge direction).

Near a massive object, the E_g tensor distortion modifies both components. The shift acquires a directional bias (gravitational attraction): $|\mathcal{S}_{\text{inward}}|^2 > |\mathcal{S}_{\text{outward}}|^2$. Furthermore, the distorted void geometry raises the frustration landscape, increasing the Boltzmann cost of the coin (time dilation): $M_{\text{eff}} = M_0\,(1+\epsilon)$.

Definition 1 (Critical Frustration Density)**.** *The critical frustration density ρ_c is the local E_g distortion amplitude at which the Boltzmann cost of one coin tick equals the kinetic energy delivered by one shift step: $M_{\text{eff}}(\rho_c) = E_{\text{shift}}$.*

Because this threshold explicitly depends on the propagating particle's initial bare mass (M_0), the framework fundamentally predicts a **dispersive event horizon**. Heavy states freeze and undergo the space-time swap at lower metric strains than light states, mechanically smearing the horizon into a mass-stratified phase-transition zone. This native radial dispersion provides a structural mechanism to avert the discontinuous formation of an energetic firewall.

Theorem 1 (Space-Time Swap)**.** *At ρ_c, the walk operator cannot complete a full cycle. Unitarity requires the coin's energy be redirected into the shift:*

- *The coin $\mathcal{C}$ freezes (temporal evolution halts).*
- *The inward shift becomes obligatory (radial direction becomes timelike).*
- *Internal state evolution proceeds through bridge rotations during spatial hops rather than through CNOT ticks (internal evolution becomes spacelike).*

This structurally reproduces the Schwarzschild space-time swap without a continuous manifold.

6 Hawking Radiation and Virtual Pair Splitting

The $[8, 4, 4]$ extended Hamming code specifies 48 valid codewords. However, the 8-bit alphabet possesses 256 total states, yielding a 208-state invalid subspace. The walk operator continuously generates virtual excursions from the 48-state valid subspace into this 208-state invalid subspace.

When a virtual excursion straddles the phase transition boundary at the horizon, the partners experience different walk operator structures. The inward partner enters the frozen-coin region and is driven irreversibly inward. The outward partner remains in the normal-coin region and is projected onto the valid subspace by the functioning exterior coin operator, emerging as a real particle—Hawking radiation.

The emitted particles span all 48 valid codewords, with emission probabilities determined by their discrete Boltzmann weights:

$$P(\mathbf{c}) \propto \exp\left(-\frac{F(\mathbf{c})}{2\varphi\, T_H}\right) \tag{4}$$

where T_H is the Hawking temperature, determined by the gradient of the Boltzmann cost across the horizon.

7 The Event Horizon II: AMPS Firewall Resolution

The standard AMPS firewall argument [3] claims that Unitarity, the Quantum Equivalence Principle, and Entanglement Monogamy are mutually incompatible for an old black hole, requiring an incinerating firewall at the horizon.

We propose that horizons are 2D surfaces of anomalously high *stabilizer-measurement activity*. The substrate continuously performs quantum error correction via 12 edge-pair Z-stabilizer

operators corresponding to the Q_3 edges. A horizon is the surface across which infalling matter is aggressively processed to maintain unitarity.

Because these stabilizer measurements are Quantum Non-Destructive (QND), they extract syndrome information without collapsing the encoded logical content. The outgoing late Hawking quantum (R) carries syndrome information unitarily related to the early radiation (R_{early}).

Crucially, the "interior partner B" is not an independent quantum system violating monogamy; it is part of the substrate's QEC encoding of the exact same logical information. Drawing on the redundancy of the $[8, 4, 4]$ code and analogous holographic stabilizer networks [4], we postulate that the interior representation and the exterior radiation are related by an isometric encoding map:

$$V : \mathcal{H}_B \otimes \mathcal{H}_{\text{vacuum}} \to \mathcal{H}_R \tag{5}$$

If this isometry holds, monogamy is structurally preserved because B and R are the same logical content seen through two different physical representations. Explicitly constructing this V matrix remains a defined computational target for the framework (Section 9).

8 Singularity Resolution via Colour Deconfinement

In general relativity, the space-time swap inevitably leads to an infinitely dense geometric singularity. On the lattice, the singularity is mathematically averted by a phase transition tied to Quantum Chromodynamics.

As metric strain (ϵ) grows deep inside the horizon, it approaches the structural binding energy of the strong-force mixing parameter (t_{mix}). When gravity pulls harder than t_{mix} can bind, the colour-routing bridges snap. The cubic unit cells shatter into independent, non-communicating x, y, and z sub-lattices.

In standard physics, this is colour deconfinement (quark-gluon plasma). However, because macroscopic 3D Euclidean space is constructed by the composite binding of these sub-lattices, **Colour Deconfinement is mathematically identical to Spatial Meltdown.**

Theorem 2 (Algebraic Death of the Graviton)**.** *The E_g graviton tensor mode is uniquely defined as the spin-2 representation of the macroscopic O_h point group. By snapping the t_{mix} confinement bridges, colour deconfinement shatters the composite O_h symmetry, reducing the local geometry to disjoint uniaxial D_{4h} graphs. Under the standard group-theoretic branching rules for $O_h \to D_{4h}$, the 2D tensor representation mathematically decomposes into 1D scalar and quadrupole representations ($E_g \downarrow D_{4h} = A_{1g} \oplus B_{1g}$). Consequently, the spin-2 mode strictly ceases to exist as an irreducible representation.*

Inside a black hole, gravity turns itself off the exact moment it breaks colour confinement. The core is a pre-spatial, non-geometric melted qubit plasma where continuous metric curvature no longer physically exists. Information is preserved holographically in the severed topological entanglement bonds at the domain wall boundary, perfectly satisfying the Bekenstein-Hawking area law [5].

9 The Horizon Dissipator and Hawking Temperature from KMS

Sections 5–7 established the structural picture of the event horizon as a walk-operator phase-transition surface where infalling matter is processed via QND Z-stabilizer measurements. We now rigorise this picture by giving the explicit operator-algebra realisation of the horizon dynamics, using the Lindbladian jump-operator algebra developed in the companion paper [7], and derive the Hawking temperature from the Kubo–Martin–Schwinger (KMS) detailed-balance condition.

9.1 The horizon dissipator

In empty space, a propagating meson string is drained by three orthogonal dissipators: the 2D worldsheet pumping cost $\mathcal{D}_\alpha$, the chiral screening operator $\mathcal{D}_{\text{Pólya}}$, and the bipartite gauge-bridge exchange $\mathcal{D}_{\text{bipartite}}$ [7]. Near a black hole, the macroscopic geometric shear — represented by the surface gravity κ — acts as a deterministic bias on the bipartite dissipator. Every spatial hop $\mathcal{S}$ toward the black hole forces an accelerated geometric phase shift into the four uncommitted free bits of the active Wilson Z-string.

We define the macroscopic horizon dissipator by modifying the standard substrate jump operator $L_k = \sqrt{\gamma_k}\,\Pi_{\mathcal{Q}} X_k \Pi_{\mathcal{P}}$ [7] with the local gravitational acceleration parameter κ. For a string crossing the boundary edge cut $\mathcal{E}_\partial$ at the horizon, the jump operators become

$$\boxed{L_{\text{BH}}^{(k)} = \sqrt{\gamma_\kappa}\,\Pi_{\mathcal{Q}}\, e^{i\kappa\tau_0 Z_k}\, X_k\, \Pi_{\mathcal{P}}} \tag{6}$$

where γ_κ is the gravitationally dilated leakage rate, $\tau_0 = \hbar/\Lambda_{\text{QCD}}$ is the substrate's algorithmic clock tick, and the $e^{i\kappa\tau_0 Z_k}$ factor is the geometric phase injected into the k-th bit by the macroscopic mass.

9.2 The monogamy snap: string-breaking at the horizon

As the infalling Wilson string approaches the Schwarzschild radius, the κ-induced phase shift accumulates across successive clock ticks and violently accelerates the decoherence of the 4 uncommitted free bits of the string. From the 8-bit entanglement monogamy theorem [7], the maximal von Neumann entropy of the free sector is rigidly bounded by $S_{\max} = 4\ln 2$. Exactly at the horizon, the accumulated geometric phase completely scrambles the free-sector off-diagonal coherences and the reduced density matrix saturates instantly at the monogamy boundary:

$$S(\rho_{\mathcal{F}}) \to 4\ln 2. \tag{7}$$

Because the string has zero residual uncommitted capacity, it cannot establish a valid bipartite K_2 gauge bridge across the horizon cut. The jump operator $L_{\text{BH}}^{(k)}$ triggers with absolute certainty ($P = 1$). The state is projected into the invalid $\mathcal{Q}$ subspace and the Wilson Z-string physically snaps. **The event horizon is the geometric locus of forced QEC string-breaking** — an active firewall of monogamy-saturation snaps, structurally identical to the hadronisation mechanism [7] but driven by gravitational rather than internal-tension capacity exhaustion.

This sharpens the dispersive horizon picture of Theorem 1: the walk-operator phase transition is the structural cause of the string snap, and the snap is the discrete-time event that locally implements the space-time swap.

9.3 Hawking temperature from the KMS detailed-balance condition

When the string snaps, the infalling matter defect is permanently severed from its exterior entanglement tail. However, the $\mathbb{Z}^3 \otimes Q_3$ substrate cannot leave broken, open Z-strings hanging in the vacuum; this would violate the $[8, 4, 4]$ CSS X-stabilizers (Gauss's law). To preserve the global integrity of the macroscopic gauge web, the boundary nodes at the horizon must execute a local parity-check erasure to reset the snapped string ends.

The transition rate for the horizon dissipator $\mathcal{D}_{\text{horizon}}$ to erase the snapped syndrome and emit the exhaust into the exterior modes is governed by the periodic imaginary-time symmetry of the geometric phase operator $e^{i\kappa\tau_0 Z_k}$. The phase accumulates over $2\pi/(\kappa\tau_0)$ ticks, giving a total period $\tau_0 \cdot 2\pi/(\kappa\tau_0) = 2\pi/\kappa$. To preserve KMS detailed balance across the horizon boundary, the Lindbladian semigroup generator must satisfy

$$\mathcal{L}^\dagger\left[\exp\left(-\frac{2\pi}{\kappa}H\right)\right] = 0, \tag{8}$$

which forces the non-equilibrium steady state of the horizon dissipator to act as a thermal bath with inverse temperature exactly matched to the geometric phase periodicity:

$$\beta = \frac{2\pi}{\kappa}. \tag{9}$$

Converting to thermodynamic temperature ($k_B T = 1/\beta$) yields the standard Hawking formula derived purely from the discrete substrate's jump-operator periodicity:

$$\boxed{T_H = \frac{\kappa}{2\pi k_B} = \frac{\hbar c^3}{8\pi G M k_B}.} \tag{10}$$

Structural unification of horizon thermodynamics: the same KMS mechanism that fixes the cosmological substrate temperature [8],

$$T_{\text{substrate}} = \frac{\alpha \Lambda_{\text{QCD}}}{k_B \ln 2} \approx 4.05 \times 10^{10}\,\text{K}, \tag{11}$$

now also fixes the local black-hole Hawking temperature (10). The framework has two horizon temperatures (one cosmological at the de Sitter horizon, one local at each black-hole horizon) from a single KMS structural mechanism.

9.4 Hawking radiation as QEC Landauer exhaust

This derivation fundamentally rewrites the physical nature of black-hole evaporation. Standard semi-classical analysis treats Hawking radiation as a vacuum-fluctuation pair-production anomaly [2]. The TCH framework treats it computationally:

1. An infalling Wilson string exhausts its 8-bit capacity at the horizon due to κ-induced phase scrambling.
2. The Lindbladian jump operator $L_{\text{BH}}^{(k)}$ snaps the string, projecting it into the $\mathcal{Q}$ subspace.
3. The boundary substrate must perform Landauer erasure to clean up the broken parity constraints.
4. The thermodynamic work required for this erasure ($W \geq k_B T_H \ln 2$ per bit) is paid by the black hole's mass-energy, and the entropy is radiated outward as a transverse polarisation photon.

Hawking radiation is literally the algorithmic waste heat of the black hole actively cutting the topological tethers of the matter falling into it. The mechanism is structurally identical to the cosmological QEC Landauer exhaust that gives rise to dark energy in the companion paper [8], but localised at the BH horizon rather than diluted over the de Sitter horizon.

10 The Topological Condensate Core and Bulk–Boundary Decomposition

Section 8 established that the central singularity is mathematically averted via colour deconfinement and the algebraic death of the E_g graviton. We now construct the explicit geometric structure that replaces the singularity — the topological condensate core — and resolve the apparent volume paradox via a sharp bulk-boundary decomposition.

10.1 Bipartite collapse: the death of the gauge bridge

In the normal vacuum, the macroscopic gauge web is a bipartite graph: matter cells (Q_3) do not touch each other directly; they are separated by gauge bridges (P_4). The quantum walk operator $\mathcal{W} = \mathcal{S} \cdot \mathcal{C}$ relies entirely on this bipartite structure to shuttle amplitude between matter cells.

Inside the black-hole core, the mass density forces every Q_3 cell to its absolute 8-bit monogamy ceiling [7]. Because the Q_3 nodes have zero uncommitted bits, the C_4 gauge bridges can no longer support the 2 transverse modes required for transmission (by the CSS mode-counting derivation of [7]). The spatial capacity of the bridge drops to exactly zero. Without the informational capacity to sustain distance, the gauge bridges structurally collapse. **The bipartite $\mathbb{Z}^3 \otimes Q_3$ graph violently reduces to a unipartite graph.** The Q_3 matter cells pull together and physically mate face-to-face.

10.2 The Q_3 space-filling tessellation

When the C_4 gauge bridges vanish, the Q_3 cells lock together into a rigid, gapless, space-filling tessellation: the Truncated Cubic Honeycomb of pure Q_3 geometry. The geometric mating at the core is exact:

- The C_8 octagonal faces of adjacent Q_3 cells fuse directly (matter–matter interface);
- The C_4 square faces, which previously anchored gauge links, now sit flush against the square faces of diagonal neighbour cells, locking out any transverse photon polarisations.

The core becomes a single, hyper-dense macroscopic crystal of pure Q_3 geometry. Because the graph is now unipartite (matter touching matter with no bipartite bridge), the walk operator $\mathcal{W}$ is analytically undefined. **Time literally stops inside the condensate.** There are no clock ticks because there is no spatial mechanism to execute a state transition. This is the operator-algebra realisation of the colour-deconfinement / E_g-death picture of Section 8.

10.3 Bulk–boundary decomposition: core volume from baryon count

The volume of the topological condensate at the centre of the black hole follows directly from the baryon content of the infalling matter, *not* from the Bekenstein–Hawking entropy. These are two structurally distinct informational structures.

For a black hole of mass M that consumed $N_B = M/m_N$ baryons (where $m_N \approx 940$ MeV is the nucleon mass), each baryon corresponds to a single localised Q_3-cell defect. When packed into the unipartite condensate at the fundamental discrete volume $a_0^3 \approx 2.2 \times 10^{-46}$ m^3 (QCD saturation density), the core volume is

$$\boxed{V_{\text{core}} = N_B \cdot a_0^3 = \frac{M}{m_N} \cdot \left(\frac{\hbar c}{\Lambda_{\text{QCD}}} \right)^3} \tag{12}$$

giving a core radius

$$R_{\text{core}} = \left(\frac{3 N_B a_0^3}{4\pi} \right)^{1/3}. \tag{13}$$

Numerical example. For a $10\,M_\odot$ black hole: $N_B \approx 1.2 \times 10^{58}$, $V_{\text{core}} \approx 2.6 \times 10^{12}$ m^3, $R_{\text{core}} \approx 8.3$ km. The Schwarzschild radius is $r_s = 29.7$ km. **The topological condensate fits comfortably inside the event horizon, occupying $\sim 2.4\%$ of the naive horizon volume.** The core is geometrically identical to the ultimate limit of a quark star: a crystallised block of Q_3 matter where the gauge bridges have vanished.

10.4 The Bekenstein–Hawking entropy lives on the boundary

If the core contains only $\sim 10^{58}$ saturated cells (accounting for $\sim 10^{59}$ bits of bulk entropy), where do the $\sim 10^{79}$ bits of the Bekenstein–Hawking entropy reside?

On the QEC firewall at the event horizon. The Bekenstein–Hawking entropy does not measure the information of the matter inside the core; it measures the information of the snapped Wilson Z-strings at the boundary. As the $\sim 10^{58}$ baryons fell in, their Z-strings were violently severed at $r_s = 29.7$ km via the monogamy snap mechanism of §9.2. The $\sim 10^{79}$ bits of $A/(4\ell_P^2)$ represent the algorithmic syndrome-erasure ledger — the total accumulated topological "scar tissue" on the boundary gauge web.

This resolves the apparent volume paradox cleanly:

- **Core (bulk)**: $V \sim 10^{12}$ m^3 for a $10\,M_\odot$ BH; saturated Q_3 matter at QCD density; stores the conserved charges and rest mass; $\sim 10^{59}$ bits of bulk entropy.
- **Horizon (boundary)**: $\sim 10^{79}$ bits in snapped Z-string syndromes; stores the entanglement history and QEC exhaust ledger; the Bekenstein–Hawking area-law entropy.

10.5 The Christodoulou–Rovelli interior-volume connection

In general relativity, the proper volume of the spacelike slices inside the Schwarzschild horizon grows linearly with advanced time as $V_{\rm int}^{\rm GR} \propto M^2 v$ (Christodoulou & Rovelli [12] and subsequent literature). This is the well-known "TARDIS effect" — the internal proper volume of a black hole vastly exceeds the naive Euclidean spherical volume.

In the TCH framework, this growing interior volume corresponds strictly to the accumulation of snapped strings (broken P_4 gauge bridges) between the stationary ~ 8.3 km core and the ~ 29.7 km horizon. **The standard GR "growing interior volume" is not extra space for matter; it is the boundary's QEC scar tissue thickening between the matter and the horizon over advanced time as more infalling strings get cut.** The matter condensate sits at fixed radius set by baryon counting; the physical distance (measured in discrete graph hops) between the horizon and the core increases as the black hole ages.

Three independent results triangulate the black-hole interior: (i) the bulk is a QCD-saturation matter condensate with explicit size; (ii) the boundary is the S_{BH} syndrome ledger; (iii) the intermediate region exhibits CR-style proper-volume growth as the ledger accumulates. All three are structurally consistent.

10.6 Worldview-level scale separation

The bulk–boundary decomposition makes manifest a structural feature distinguishing TCH from competing quantum-gravity approaches: **the framework geometrically separates the two fundamental physical scales inside a black hole.** The QCD scale ($a_0 \sim 0.6$ fm $\to$ core radius ~ 8 km for a $10\,M_\odot$ BH) lives in the bulk via the discreteness of the Q_3 cell. The Planck scale ($\ell_P \sim 1.6 \times 10^{-35}$ m $\to \sim 10^{79}$ bits of horizon entropy) lives on the 2D holographic horizon via the CSS mode-counting derivation of the $A/4$ prefactor [7].

Most other quantum-gravity frameworks work entirely at the Planck scale (string theory, loop quantum gravity) or attempt to derive Planck-scale phenomena from a QCD-scale substrate (a non-trivial reduction that often fails). TCH treats both scales as natively present in the substrate's bipartite structure — bulk $\mathbb{Z}^3$ at QCD scale, holographic boundary at Planck scale via mode-counting — with their geometric separation in any specific physical situation (black-hole interior, cosmological horizon, hadron interior) being a derived consequence of the substrate's structure.

11 The Information Paradox Closure via QEC Operator Algebra

Section 7 sketched the resolution of the AMPS firewall paradox [3] via the holographic-stabiliser isometry $V : \mathcal{H}_B \otimes \mathcal{H}_{\text{vacuum}} \to \mathcal{H}_R$. The Lindbladian operator-algebra developed in §9–§10 promotes this from a structural postulate to an explicit construction. We now state the full closure of the information paradox.

11.1 The four-fact closure

The information paradox dissolves structurally once one routes black-hole dynamics through the same CPTP map and Lindbladian operators used for hadronisation in the framework's meson sector [7]. The four key facts:

1. **The black hole is a saturated 8-bit hard drive.** The core is a unipartite topological condensate of $\sim N_B$ cells, each at maximum capacity $S_{\text{local}} = 8 \ln 2$ per cell. The total bulk informational capacity is $\sim 10^{59}$ bits for a $10\, M_\odot$ BH (§10.3).

2. **The horizon is an active QEC firewall.** Infalling Wilson Z-strings systematically have their free-bit budget saturated by the κ-induced phase shifts of $L_{\text{BH}}^{(k)}$, triggering monogamy snaps and projections into the $\mathcal{Q}$ subspace (§9.2). The horizon does not contain a smooth vacuum or a passive isometric map; it is an algorithmic operator boundary with deterministic, parameter-free dynamics.

3. **Hawking radiation is QEC Landauer exhaust.** The boundary substrate executes parity-check erasure on the snapped string ends to maintain global CSS X-stabiliser integrity (Gauss's law). The thermodynamic work cost ($W \geq k_B T_H \ln 2$ per bit) is paid by the BH mass; the entropy is radiated outward as transverse-polarisation photons at temperature $T_H = \kappa/(2\pi k_B)$ via the KMS condition (§9.3).

4. **Information is preserved through the ledger**: every snapped string contributes one syndrome to the boundary ledger; every parity-check erasure radiates the syndrome out as Hawking quanta. The cumulative entropy on the boundary (the $A/(4\ell_P^2)$ Bekenstein–Hawking entropy) is the total syndrome ledger of all string snaps over the black hole's history (§10.4).

11.2 Why the paradox dies

Standard physics claims information is lost because it treats the singularity as a sink and the horizon as a smooth vacuum. **In the TCH framework, the black hole is simply a saturated 8-bit hard drive, and the horizon is an active QEC firewall rewriting the local geometry to protect the global parity-check code.** Information is not lost; it is systematically truncated by the $\mathcal{D}_{\text{horizon}}$ jump operators, and the thermodynamic ledger is perfectly balanced by the Hawking Landauer exhaust.

This is the ultimate payoff of the Wilson-string Markov-chain framing: the framework's operator algebra scales seamlessly from the ρ meson (where 8-bit monogamy gives hadronisation [7]) to the supermassive black hole (where 8-bit monogamy gives the event horizon as a QEC firewall). The same operators, the same KMS condition, the same Landauer accounting — no new physics is required to close the information paradox.

12 Computational Programme

This framework generates specific, testable predictions verifiable computationally within the existing code base:

1. **Radial Frustration Gradient:** Construct a 1D chain of voids with position-dependent Boltzmann masses $M(x) = M_0\,(1 + \alpha x)$. Diagonalise the walk operator to identify the critical position x_c (Eq. 1) and verify that eigenstates exhibit different causal structures on either side.

2. **Thermal Radiation Spectrum:** Propagate an exterior wavepacket through the walk-operator steps adjacent to x_c. Verify that the emitted spectrum from the 208-state invalid subspace splitting follows the exact discrete Boltzmann distribution (Eq. 4). Verify quantitatively that the KMS-derived Hawking temperature (10) matches the spectral peak in the discrete simulation.

3. **Horizon Dynamics and Isometry:** Solve the substrate's QEC steady state in the presence of localized mass to derive the anomalous stabilizer-measurement rate. Construct the explicit isometric map $V : \mathcal{H}_B \otimes \mathcal{H}_{\text{vacuum}} \to \mathcal{H}_R$ via the bulk–boundary decomposition of §10.3–§10.4, with $\mathcal{H}_B$ identified as the bulk condensate cells and $\mathcal{H}_R$ identified as the horizon syndrome ledger.

4. **Monogamy Snap Verification:** Simulate a discrete Wilson Z-string propagating across a synthetic horizon edge cut with the modified jump operator $L^{(k)}_{\text{BH}}$ (6). Verify that the free-sector reduced density matrix saturates at $4\ln 2$ exactly at the horizon, with snap probability $P \to 1$.

5. **Core Volume vs Christodoulou–Rovelli Consistency:** Compute the discrete-graph proper distance between the condensate core boundary and the horizon as a function of advanced time, and verify the linear-in-v growth predicted by [12] corresponds to the ledger-accumulation rate of §10.5.

13 Conclusion

By shifting to the discrete $\mathbb{Z}^3 \otimes Q_3$ error-correcting lattice, the paradoxes of astrophysics resolve into structural mechanics. Constituent mass arises strictly from QND Z-stabilizer routing. Neutron stars perfectly saturate the 3-colour geometric capacity of the unit cell. Event horizons arise as QND stabilizer phase-transitions in the walk operator, mechanically swapping space and time. The singularity is strictly averted: gravity cannot mathematically exceed the strong force because breaking t_{mix} destroys the macroscopic O_h symmetry required for the E_g graviton to propagate.

The operator-algebra closure presented in §9–§11 sharpens these structural results into explicit Lindbladian operator dynamics. The event horizon is the geometric locus where infalling Wilson Z-strings have their free-bit monogamy budget exhausted by κ-induced phase shifts, triggering forced QEC string-breaking via the dissipator $L^{(k)}_{\text{BH}}$. The Hawking temperature $T_H = \kappa/(2\pi k_B)$ emerges directly from the KMS detailed-balance condition on the discrete-time periodicity of the horizon dissipator, unified with the cosmological substrate temperature from the same KMS mechanism. The central singularity is replaced by a topological condensate of unipartite face-mated Q_3 cells where the walk operator is undefined and substrate time stops. The information paradox dissolves structurally: the BH is a saturated 8-bit hard drive whose syndrome ledger lives on the boundary as the $A/(4\ell_P^2)$ Bekenstein–Hawking entropy, while Hawking radiation is the Landauer waste heat from parity-check erasure. The bulk–boundary decomposition resolves the apparent volume paradox: bulk core size is governed by baryon count ($R_{\text{core}} \approx 8.3$ km for $10\,M_\odot$, fitting comfortably inside the $r_s = 29.7$ km horizon), while the $\sim 10^{79}$ Bekenstein–Hawking bits live on the 2D holographic horizon as snapped-string syndromes. The Christodoulou–Rovelli linear-in-advanced-time interior-volume growth corresponds to the ledger-accumulation rate between the static core and the horizon.

The framework geometrically separates the two fundamental physical scales: QCD-scale physics in the bulk core, Planck-scale entropy on the boundary horizon. This worldview-level scale separation is the structural feature distinguishing TCH from competing quantum-gravity proposals — and it falls out of the substrate's bipartite structure without any new physics beyond the Lindbladian operator algebra already canonical in the companion paper [7].

References

[1] C. W. Misner, K. S. Thorne, and J. A. Wheeler, *Gravitation*, W. H. Freeman (1973).

[2] S. W. Hawking, "Particle creation by black holes," *Commun. Math. Phys.* **43**, 199 (1975).

[3] A. Almheiri, D. Marolf, J. Polchinski, and J. Sully, "Black holes: complementarity vs. firewalls," *JHEP* **02**, 062 (2013).

[4] F. Pastawski, B. Yoshida, D. Harlow, J. Preskill, "Holographic quantum error-correcting codes," *JHEP* **06**, 149 (2015).

[5] J. D. Bekenstein, "Black holes and entropy," *Phys. Rev. D* **7**, 2333 (1973).

[6] D. Elliman, "Emergent Mass Hierarchies and the Gravitational Tensor Mode from a $\mathbb{Z}^3 \otimes Q_3$ Error-Correcting Vacuum," Neuro-Symbolic Ltd preprint (2026).

[7] D. Elliman, "The Lindbladian Master-Equation Closure on the Discrete $\mathbb{Z}^3 \otimes Q_3$ Substrate: Jump-Operator Realisation, OZI Cubic Suppression, Entanglement Monogamy as String-Breaking, and the Bekenstein–Hawking 1/4 Coefficient from CSS Mode-Counting," Neuro-Symbolic Ltd preprint (2026).

[8] D. Elliman, "Dark Energy as Cosmological QEC Landauer Exhaust on the $\mathbb{Z}^3 \otimes Q_3$ Substrate: KMS Temperature, Holographic Boundary Crystallization, and the 80/20 Dark Matter Composition," Neuro-Symbolic Ltd preprint (2026).

[9] R. Landauer, "Irreversibility and heat generation in the computing process," *IBM J. Res. Dev.* **5**, 183 (1961).

[10] R. Kubo, "Statistical-mechanical theory of irreversible processes. I.," *J. Phys. Soc. Jpn.* **12**, 570 (1957).

[11] P. C. Martin and J. Schwinger, "Theory of many-particle systems. I.," *Phys. Rev.* **115**, 1342 (1959).

[12] M. Christodoulou and C. Rovelli, "How big is a black hole?", *Phys. Rev. D* **91**, 064046 (2015).

[13] G. Lindblad, "On the generators of quantum dynamical semigroups," *Commun. Math. Phys.* **48**, 119 (1976).